A TWO STEP PREDICTOR-CORRECTOR METHOD FOR VOLTAGE COLLAPSE POINT ESTIMATION

By

Anas Yousif Ahmed Ali

Abdelrahman A. Karrar
Associate Professor of Electrical Engineering
Committee Chair

Ahmed H. Eltom
Professor of Electrical Engineering
Committee Member

Gary L. Kobet
Adjunct Professor of Electrical Engineering
Committee Member

A TWO STEP PREDICTOR-CORRECTOR METHOD FOR VOLTAGE COLLAPSE POINT ESTIMATION

By

Anas Yousif Ahmed Ali

A Thesis Submitted to the Faculty of the University of
Tennessee at Chattanooga in Partial
Fulfillment of the Requirements of the Degree of
Master of Science: Engineering

The University of Tennessee at Chattanooga
Chattanooga, Tennessee

May 2019

Copyright © 2019

By Anas Yousif Ahmed Ali

All Rights Reserved

ABSTRACT

Voltage Collapse is the system failure to obtain acceptable voltage levels in significant part of the power system, and it is often due to system failure to satisfy reactive power demand. Voltage Collapse can lead to blackout like the one occurred in 2003 in North America. Methods for on-line voltage stability monitoring were established, and indices to quantify it were proposed. However, estimations of voltage collapse point based on these indices are often inaccurate or time consuming. A well-established method of voltage collapse point estimation is the Continuation Power Flow (CPF). CPF is considered accurate but, it is very computationally expensive for large systems.

This work aims to speed up the predictor-corrector process by using a VSI called P-index. An initial prediction is made, corrected using a continuation technique, and then updated after correction. The results are relatively accurate and it makes a significant improvement to the CPF computational time.

.

TABLE OF CONTENTS

LIST OF TABLES

LIST OF FIGURES

CHAPTER 1

INTRODUCTION

1.1 Overview

Monitoring voltage stability is one of the biggest tasks of power system operations. This task has never been more important as the electric demand growth is rapidly growing worldwide, and incidents where problems with voltage stability have led to wide range blackouts. Several Voltage Stability Indices (VSI) have been developed to quantifiably monitor voltage stability. The point of voltage collapse can be predicted using these VSI. Another way to predict the point of voltage collapse is the Continuation Power Flow (CPF).

1.2 Problem Statement

Voltage Stability Indices based point of voltage collapse predictions are in many cases inaccurate or computationally expensive. On the other hand, continuation power flow based predictions are generally more accurate but, it is very computationally taxing. Point of voltage collapse prediction methods that are both accurate and computationally inexpensive are yet to be developed.

1.3 Objective

The main objective of this work is to use a VSI called the P-index, along with a continuation technique similar to the one used in the continuation power flow to give a prediction of the point of voltage collapse that is accurate and computationally inexpensive.

1.4 Thesis Layout

This thesis is organized as follows:

- Chapter II: This chapter provides an overview of the voltage stability problem and different voltage stability analysis tools.
- Chapter III: This chapter introduces the concepts behind the proposed methods along with the derivation of their formulas.
- Chapter IV: This chapter presents the simulation results when testing the proposed methods on different test systems. It also presents performance comparisons between the proposed methods and other voltage stability analysis tools.
- Chapter V: This chapter concludes the contributions and findings of this work. Moreover, it provides some aspects of improvement that can be investigated.

CHAPTER 2

LITERATURE REVIEW

2.1 Voltage Stability

IEEE/CIGRE Joint Task Force on Stability Terms and Definitions defines voltage stability as “the ability of a power system to maintain steady voltages at all buses in the system after being subjected to a disturbance from a given initial operating condition” [1]. Voltage instability can occur due to multiple factors, but the major ones are generation limits, transmission limits, and load dynamics [2].

In some cases a sequence of events can results in an instability called Voltage Collapse which can often be a system wide problem. IEEE/CIGRE Joint Task Force mentioned above defines voltage collapse as “the process by which the sequence of events accompanying voltage instability leads to a blackout or abnormally low voltages in a significant part of the power system” [1]. If the system is operating near its optimal operating point, voltage collapse can lead to a blackout [2].

Multiple blackout events worldwide have occurred due to voltage collapse, which have affected millions of customers. One of the most famous ones is the one happened in August 2003 in the northeastern grid of the United States and Canada which affected 50 million people [3]. Another occurred in November 2009 in Brazil which affected 60 million people [4].

The severity of impact that a voltage collapse can have on a power system, and the frequency of its occurrence has made its study an active area of research.

Voltage stability can be broadly studied under two conditions: large disturbance, and small disturbance. The first condition studies the voltage stability problem after a small disturbance to a system such as a gradual increase in load. In the latter conditions, systems' ability to maintain its voltage stability following disturbance such as faults or loss of generation unit is studied. This study is usually carried out using nonlinear time domain methods. However, linearized system dynamic equations are used to study the small disturbance [5]. Despite the dynamic nature of the problem it is usually analyzed using static methods as they allow a wider range of system conditions to be examined. Proximity to the point of collapse, and loadability margin are among the main interests of voltage stability studies.

2.2 Mathematical Formulation Voltage Instability Problem

Consider the simple radial system illustrated in figure 2.1. It shows a load Z_D that draws a power from a constant voltage source E_s through a transmission line Z_L. The active power that is drawn by the load is given by

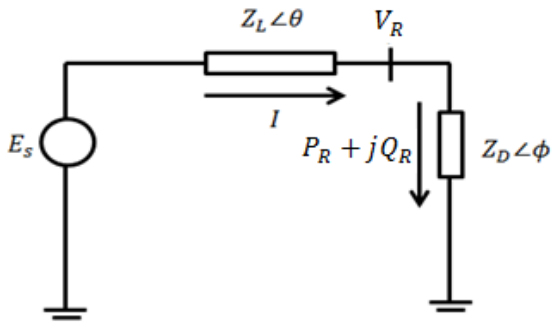

Figure 2.1 Simple Radial System to Illustrate Voltage Stability Problem

$$P_R = V_R I cos\phi \tag{2.1}$$

While the receiving end voltage V_R is given by

$$V_R = Z_D I \tag{2.2}$$

And the current I is given by

$$I = \frac{E_s}{\sqrt{(Z_L cos\theta + Z_D cos\phi)^2 + (Z_L sin\theta + Z_D sin\phi)^2}} \tag{2.3}$$

Equations 2.1 - 2.3 shows that the power drawn by the load has two competing factors that control how it changes. For a constant power factor x; a change in load magnitude results a change in both current and load voltage. The winner of these two factors depends on the ratio between the load impedance and the transmission line impedance Z_L/Z_D. Figure 2.2 below demonstrate these characteristics for normalized power and current.

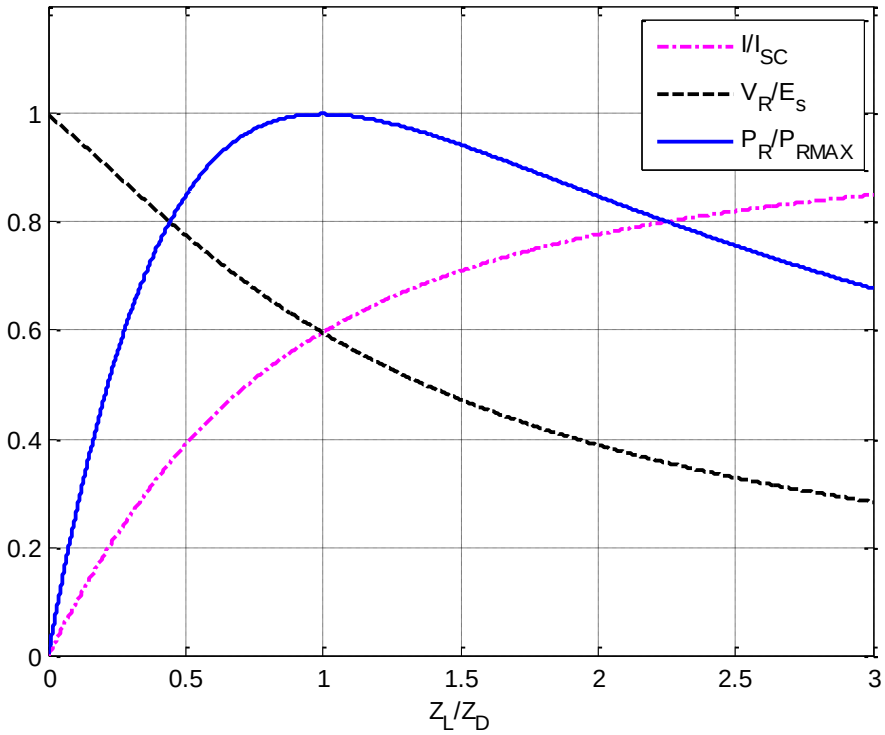

Figure 2.2 Normalized Current, Receiving End Voltage, and Reciving End Power Characteristics

As evident from the figure, the receiving end power increase as the load increases (i.e. $Z_D$decreases) until it reaches the maximum at $Z_L/Z_D = 1$. After that the trend changes and the receiving end power decreases as the load increases. After the maximum point the system becomes unstable, because an increase in load will results in a decrease in power which can lead to progressive decrease in voltage, depending on the load model characteristics [5].

2.3 Voltage – Power Characteristics

The characteristic of the voltage of a particular load bus as a function of active power is one of the most important relationships in voltage stability studies. This characteristic is often demonstrated through a curve that is called the nose curve. An example of a typical nose curve for a constant

power factor is shown in figure 2.3. As shown in the figure, the curve has two parts; stable and unstable regions. As the load power increases, the voltage drops slightly until it approaches the maximum power point. This tip of the nose curve is known as the stability limit point or the point of collapse. As the system approaches the point of collapse, the dip in voltage due to the increase of load power increases rapidly and approaches infinity at the point of collapse. After that the system enters the unstable region and load power starts to decrease instead of increasing. It is worth mentioning that load power is usually expressed as a multiple of base load, and likewise the point of collapse is expressed as the maximum multiple of base load. This multiplier is called the loading parameter or multiplier λ.

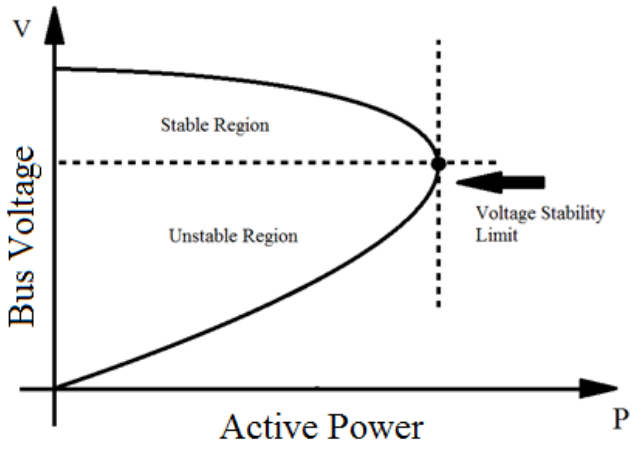

Figure 2.3 Typical Nose Curve

2.4 Voltage Collapse Mechanism

Voltage Collapse can occur through multiple processes. However, large amount of cases follow a typical scenario often evolves successive operations of On-Load-Tap-Changer

Transformer. Consider the OLTC transformer in figure 2.4. Connecting an additional load on the secondary side will lower the voltage there, which will trigger a tap change operation. If this operation kept the primary voltage constant it would have been successful. However, the operation will results in voltage drop on the primary side.

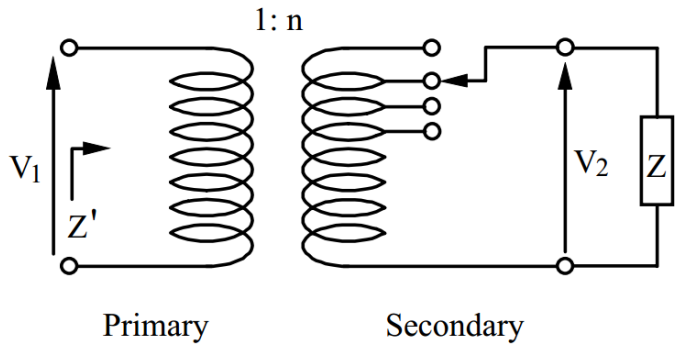

Figure 2.4 OLTC Transformer

If the reactive power demand is below the generators limits, the voltage at the generator terminal will be controlled by the AVR and the primary side of the OLTC transformer will return to the operating point before the disturbance. However, if the reactive power demand exceeds generators limits, the over excitation limiter will hold the field current constant and the generators terminal voltage will not be controlled by the AVR anymore. Hence, the voltage at the primary of the OLTC transformer will decrease causing another tap changing operation. This chain of events will repeat itself, making a successive voltage depression that can yield unacceptable voltage levels [5, 6].

2.5 The Continuation Power Flow

The voltage of a particular bus in a power system can be obtained for a specific loading parameter using power flow analysis. However, as the system approaches the point of collapse, the Jacobian matrix of the classical load flow analysis becomes singular. To overcome this problem the power flow equations are changed slightly and a continuation technique that is locally parameterized is used. This iterative process is called The Continuation Power Flow [7].

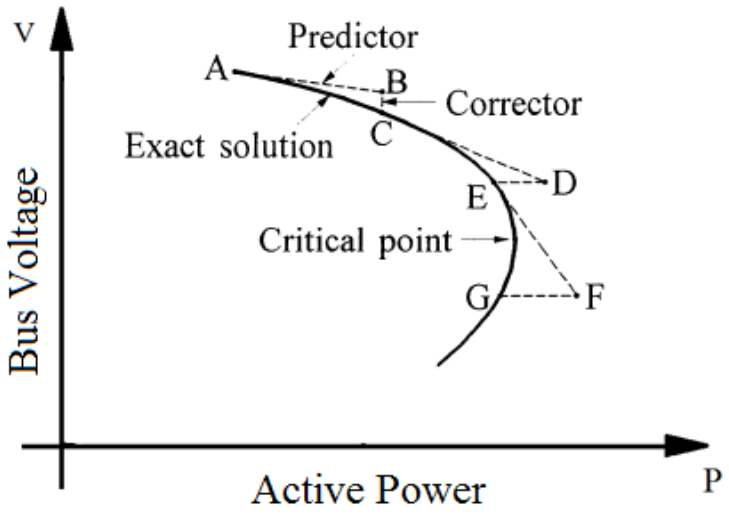

Figure 2.5 Continuation Power Flow

The general procedure of the continuation power flow is dissected to two steps at each iteration; predictor and corrector. In the predictor step, starting from a known solution a prediction of the next solution is obtained along the tangent vector of the current solution corresponding to

another loading parameter. In the correction step, the obtained prediction is corrected using conventional power flow technique. This procedure is iterated until a nose curve is fully drawn. Figure 2.5 illustrates this procedure.

To prepare the conventional load flow equation for the continuation power flow, the loading parameter is introduced as an additional state variable. The resulting equations can be written as:

$$F(\theta, V, \lambda) = 0 \tag{2.4}$$

As mentioned above the predictor predicts the next solution in the direction of the tangent vector. Tangent vector can be obtained by taking to derivative of 2.4

$$dF = F_\theta d\theta + F_V dV + F_\lambda d\lambda = 0 \tag{2.5}$$

Putting 2.5 in matrix form yields

$$[F_\theta \quad F_V \quad F_\lambda] \begin{bmatrix} d\theta \\ dV \\ d\lambda \end{bmatrix} = 0 \tag{2.6}$$

The column vector in 2.6 is the desired tangent vector, while the row vector is obtained by adding a row and a column to the conventional Jacobian matrix. The new row and column correspond to the loading parameter as it was introduced as an additional state variable. Equation 2.6 can be solved then by assigning a non-zero value (typically ± 1) to one of the components of the tangent vector. The variable which corresponds to this component is called the continuation parameter. The method of choosing this parameter will be discussed later.

$$\begin{bmatrix} F_\theta & F_V & F_\lambda \\ & e_k & \end{bmatrix} \begin{bmatrix} d\theta \\ dV \\ d\lambda \end{bmatrix} = \begin{bmatrix} 0 \\ \pm 1 \end{bmatrix} \tag{2.7}$$

Where e_k is a row vector that has suitable dimensions, and all its elements are zero except for that corresponding to the continuation parameter which is set to 1.

After obtaining the tangent vector, the next solution can be predicted as

$$\begin{bmatrix} \theta \\ V \\ \lambda \end{bmatrix} = \begin{bmatrix} \theta_o \\ V_o \\ \lambda_o \end{bmatrix} + \sigma \begin{bmatrix} d\theta \\ dV \\ d\lambda \end{bmatrix} \quad 2.8$$

The step size σ is set to a value that allows the correction procedure to converge.

In the correction step, an additional equation is added to the conventional power flow equations. In this equation, the change in continuation parameter is set to zero. Then this set of equation is solved using conventional power flow technique.

$$\begin{bmatrix} F(\theta, V, \lambda) \\ x_k - \eta \end{bmatrix} = [0] \quad 2.9$$

Where x_k represents the chosen continuation parameter and η is its predicted value. This modification of the conventional power flow equations makes the Jacobian matrix non-singular at the point of collapse.

The continuation parameter can be chosen to be the state variable with the biggest tangent vector component, i.e. the state variable that has the biggest rate of change near the given solution. The initial continuation parameter can be chosen to be loading parameter [7].

2.6 Voltage Stability Assessments Based on Thevenin Tracking

Thevenin Tracking is the voltage stability analysis method that simplifies the whole system into a Thevenin equivalent using local measurement. To demonstrate the basic concept, consider the system in figure 2.6. The figure shows the concerned load bus and the rest of the system is represented by its Thevenin equivalent.

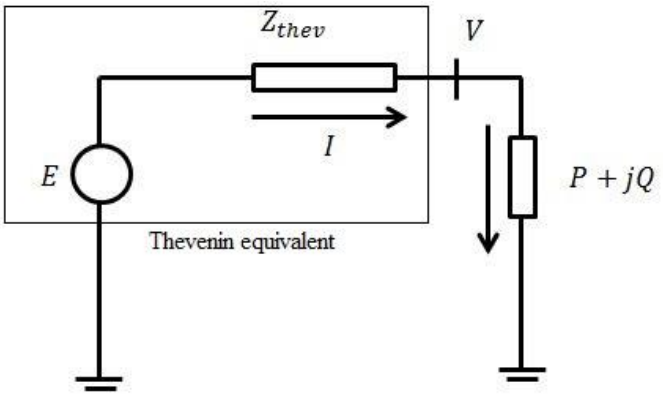

Figure 2.6 Thevenin Equivalent Example System

By equating the currents at the receiving and ending ends we obtain

$$\frac{P + jQ}{\bar{V}} = \left(\frac{\bar{E} - \bar{V}}{\overline{Z_{thev}}}\right)^* \tag{2.10}$$

This can be rearranged to obtain the following equation

$$(P + jQ)\,\overline{Z_{thev}}^* = \bar{V}(\bar{E} - \bar{V})^* \tag{2.11}$$

Equation 2.11 is quadratic, hence it has two solutions. At the point of collapse (i.e. max power transfer) these two solutions become one. So, at the point of collapse

$$\bar{V} = (\bar{E} - \bar{V})^* \quad 2.12$$

Or

$$\left|\overline{Z_{app}}\right| = |\overline{Z_{thev}}| \quad 2.13$$

Where $\overline{Z_{app}}$ is the ratio between the voltage and current obtained from the local measurement at the concerned bus. This method tracks the present time $\overline{Z_{app}}$ to the Thevenin impedance and uses it as an assessment of proximity to voltage collapse [8].

This method has an inherent flaw which is reducing a complex and non-linear discontinuous power system to a simple Thevenin equivalence and the analysis of a multi-dimensional problem from a single load only. It is difficult to develop a precise and accurate algorithm that allows optimal utilization of the system. Conservative algorithms can lead to underutilization of system which is not favorable since the existing power systems need to operate near its limits to satisfy the ever growing demand. On the other hand if algorithms were not careful enough, dangerous situations can arise, which can lead to potential problems that can cost utilities a large amount of money. Also reducing the system to an equivalent basic Thevenin circuit ignores important parameters like generation limits.

There are some other technical issues as well such as the wideness of the time window that the measurements are gathered in. The time window should be wide enough for the operating conditions to change, but narrow enough to satisfy the constant Thevenin impedance assumption. For example for a contingency or a sudden large load change can change the Thevenin equivalent network parameters that represent the system side in the selected window. This could lead to a great inaccuracy in indices.

Another issue arises when the schedule of generators that are electrically distant is changed. This change may not affect the measurements, and since the scheduling of generators also determines the voltage stability of the system, this can lead to a considerable error in indices estimation. This is because the measurement based approach cannot perform a predictive based analysis, which is due the system linearization at the equilibrium point and all the calculations are based upon the measurements available at that instant.

2.7 Voltage Stability Indicators for Power Systems

To assess the voltage stability of the system quantitatively, multiple Voltage Stability Indices have been developed. A Voltage Stability Index (VSI) is a scalar number that quantitatively describes the voltage stability condition of the system and can be monitored as system parameters change [9]. The following sections present some of these indices.

2.7.1 The Second Order Index

This index is a Jacobian matrix based VSI that uses maximum singular value of the inverse of the Jacobian matrix σ_{max} along with its derivative with respect system load variation C_{tot} to assess the system voltage stability. The index is given by:

$$i = \frac{1}{i_0} \frac{\sigma_{max}}{\frac{d\sigma_{max}}{dC_{tot}}} \tag{2.14}$$

Where i_0 is the ratio between σ_{max} and $d\sigma_{max} \,/\, dC_{tot}$ at base load.

Unlike the index proposed at [10] this index has a linear trend. This linearity makes it very useful in point of collapse and loadability margin assessment [11]. On the other hand, its need to process and manipulate very large matrices makes it very computationally expensive.

2.7.2 The Tangent Vector Index

The Tangent Vector Index is another Jacobian matrix based VSI that uses system tangent vector to assess the system voltage stability. The Tangent Vector Index is defined as

$$TVI_i = \left|\frac{dV_i}{d\lambda}\right|^{-1} \tag{2.15}$$

Where $\frac{dV_i}{d\lambda}$ is the critical bus voltage magnitude entry in the tangent vector [12].

This index is based on the idea that the tangent vector approaches infinity as the system move closer and closer to the point of collapse. However, different systems have different tangent vectors for the same distance to collapse; this makes this index not reliable in the assessment of absolute stability.

2.7.3 The L-index:

The L index is one of the most popular voltage stability indices. It uses load flow results to assess the system voltage stability. The L index is defined as:

$$L_j = \left|1 + \frac{V_{0j}}{V_j}\right| \tag{2.16}$$

Where $\underline{V_{0j}}$ is the no-load voltage at the concerned bus j. $\underline{V_{0j}}$ is calculated as

$$V_{0j} = -\sum_{i \in G} F_{ij} \cdot V_{\mathrm{i}} \qquad 2.17$$

Where F_{ij} can be calculated from the system admittance matrix (Y-matrix) as follows:

$$F_{ij} = -[Y_{LL}]^{-1}[Y_{LG}] \qquad 2.18$$

As the load at a consumer bus increases, the L index increases until it reaches 1 at the point of voltage collapse. Hence, buses with higher L index are the weakest [13].

The main drawback of the L-index is that it is based on a two-bus system and its expansion to an n-bus system is only by analogy and not robust [14].

2.7.4 The P-index:

The P-index is a bus-based multi-bus online voltage stability monitoring index. It based on the relationship between a small change in active power and a small change in voltage. To demonstrate the concept, consider a simple radial two-bus system shown in figure 2.6. The relationship between load power and load conductance is given by:

$$G_L = \frac{P_L}{V^2}, \qquad B_L = \frac{Q_L}{V^2} \qquad 2.19$$

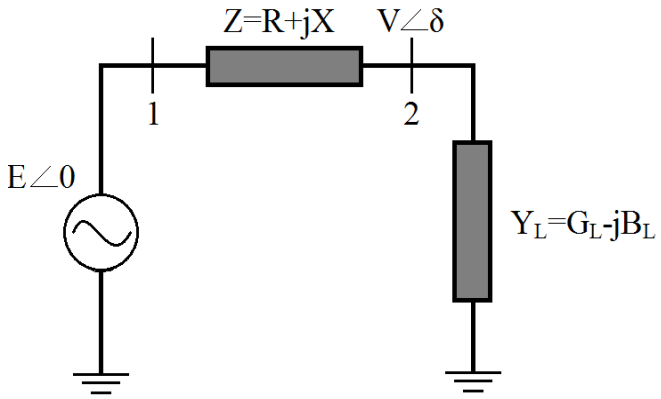

Figure 2.7 Simple Radial Two-Bus System

Now a change ΔP in load active power can expressed using 2.19 as:

$$\begin{aligned}\Delta P_L &= (V+\Delta V)^2(G_L+\Delta G_L) - V^2 G_L \\ &= (V+\Delta V)^2 \Delta G_L + (2V+\Delta V) G_L \Delta V\end{aligned} \qquad 2.20$$

This expression shows that the change in load active power arises from two factors. The first one is from connection of extra load (ΔG_L) to the bus, and the second one is from change in voltage (ΔV). This agrees with what was discussed in 2.2, and the maximum power is delivered at the collapse point, where the two opposing factors become equal. It is worth mentioning that the first factor is a gain in power due to an extra load, while the second factor is a loss of power due to the reduction of voltage.

The P-index is defined as the limiting case of the ratio between these two opposing terms, i.e. the ratio of the lost power to the gained one, as the change in load and voltage become infinitesimal:

$$P_{index} = \lim_{\Delta V, \Delta G_L \to 0} -\frac{(2V+\Delta V)G_L}{(V+\Delta V)^2} \cdot \frac{\Delta V}{\Delta G_L} = -\frac{2G_L}{V} \cdot \frac{dV}{dG_L} \qquad 2.21$$

The rate of change in voltage with respect to load conductance $\frac{dV}{dG_L}$ can be replaced by the more suitable and commonly used term in network terminology $\frac{dV}{dP_L}$ as follows:

$$\frac{dV}{dG_L} = \frac{dV}{dP_L} \cdot \frac{dP_L}{dG_L} \tag{2.22}$$

From 2.19 it can be stated that:

$$dP_L = V^2 dG_L + 2VG_L dV \tag{2.23}$$

And:

$$\frac{dP_L}{dG_L} = V^2 + 2VG_L \frac{dV}{dG_L} \tag{2.24}$$

Now Substituting in 2.22:

$$\frac{dV}{dG_L} = \frac{dV}{dP_L}\left(V^2 + 2VG_L \frac{dV}{dG_L}\right) \tag{2.25}$$

Equation 2.25 can be manipulated to be:

$$\frac{dV}{dG_L} = \frac{V^2 \frac{dV}{dP_L}}{1 - 2VG_L \frac{dV}{dP_L}} \tag{2.26}$$

Substituting 2.26 in equation 2.21:

$$P_{index} = \frac{-2VG_L \frac{dV}{dP_L}}{1 - 2VG_L \frac{dV}{dP_L}} \quad 2.27$$

Using 2.19, the P-index can be expressed in terms of the load active power as follows:

$$P_{index} = \frac{-2\frac{P_L}{V}\frac{dV}{dP_L}}{1 - 2\frac{P_L}{V}\frac{dV}{dP_L}} \quad 2.28$$

The P-index is a normalized index, and its value ranges between 0 (no load conditions of the system) and 1 (voltage collapse point). This characteristic makes it simpler to monitor the voltage stability and to identify critical nodes of the system [14].

2.8 Direct Computation of the Voltage Collapse Point

Another approach to point of collapse assessment is by reformulating the problem as a constrained optimization problem. In [15] a mathematical tool called the Dog-leg Trust Region was used to solve this constrained optimization problem. This effort yielded very accurate results. However, as the system grows larger, the computation time becomes very large.

2.9 Distance to Voltage Collapse Using the P-Index

Another method used to estimate the point of collapse is proposed in [16]. This method uses the P-index discussed in 2.6.4, and assumes a quadratic relationship between load bus voltage

V and load conductance G_L. Using the simple system in figure 2.6 a relationship between V and G_L can be expressed as

$$V = \frac{a}{\sqrt{1 + bG_L + cG_L^2}} \tag{2.29}$$

Where a, b and c are constant. These constant can be calculated using the system initial condition, first, and second derivative of V with respect to G_L.

As shown in [15] the conductance at the point of collapse is calculated by

$$G_{Lm} = \frac{1}{\sqrt{c}} \tag{2.30}$$

Using 2.29 the voltage at the point of collapse V_m can be obtained. The power of the point of collapse (i.e. maximum power) P_m can also be obtained using 2.19. This result in

$$P_m = V_m^2 G_{Lm} \tag{2.31}$$

And

$$\lambda_m = \frac{V_m^2 G_{Lm}}{P_0} \tag{2.32}$$

Where λ_m the maximum is load multiplier and P_0 is the initial loading.

CHAPTER 3

METHODOLOGY

The methods proposed in this work uses two steps to estimate the voltage collapse point. From a starting point it predicts the point of collapse assuming a linear voltage-conductance relationship. This prediction is then corrected to a point on the nose curve using a continuation process similar to the one in the CPF method. Lastly this point is taken as the starting point and another prediction is made using two methods. One method uses same formula used in the first prediction, and the other one uses the voltage-conductance formula discussed in 2.8.

3.1 Voltage Collapse Point Initial Prediction

Starting from the simple system in figure 2.6 the voltage at the load bus can be given by:

$$\bar{V} = \bar{E} - \frac{\bar{E}}{\frac{1}{\bar{Y}_L} + \bar{Z}} \cdot \bar{Z} \qquad 3.1$$

Where:

$\bar{Z} = R + jX$, and $\bar{Y}_L = G_L - jB_L = G_L(1 - j \cdot tan\phi)$

For small ($\bar{Y}_L$) and ($\bar{Z}$) equation 3.1 can be approximated to:

$$\bar{V} = \bar{E} - \bar{E}\bar{Z}\bar{Y}_L \tag{3.2}$$

The voltage magnitude for a lossless line, constant load power factor, and a negligible imaginary part:

$$\begin{aligned} V &= |\bar{E} - j\bar{E}XG_L(1 - jtan\phi)| = |\bar{E}(1 - XG_L tan\phi) - j\bar{E}XG_L| \\ &\approx E(1 - XG_L tan\phi) \end{aligned} \tag{3.3}$$

Taking the derivative of this voltage relationship with respect to the load conductance:

$$\frac{dV}{dG_L} \approx -EXtan\phi \tag{3.4}$$

This analysis along with its approximations suggests a linear relationship between V and G_L. The linear relationship between V and G_L can be expressed as

$$V = aG_L + b \tag{3.5}$$

Where

$$a = \frac{dV}{dG_L} \tag{3.6}$$

and b is a constant that can be calculated from the system conditions at a known point [14]. This work calculates b at the point where the P-index is 0.5, and uses this point as the starting point of the prediction.

$$b = V_{(Pidx=0.5)} - \frac{dV}{dG_L} G_{L_{(Pidx=0.5)}} \tag{3.7}$$

As discussed in [13], the P-index at the point of collapse is 1.0. Plugging this into equation 2.19 gives

$$\bar{V} = -2aG_L \tag{3.8}$$

Solving 3.6 and 3.7 gives

$$G_L = -\frac{b}{3a} \tag{3.9}$$

and more importantly

$$V = \frac{2}{3}b \tag{3.10}$$

Equation 3.10 gives a prediction for the voltage at the point of collapse. To obtain the loading at the point of collapse, voltage and load conductance are plugged into equation 2.17.

$$P_{Lmax} = V^2 G_L = -\frac{4b^3}{27a} \tag{3.11}$$

Inserting equation 3.6 and 3.7 into equation 3.11 gives

$$P_{Lmax} = -\frac{4(V_{(Pidx=0.5)} - \frac{dV}{dG_L} G_{L_{(Pidx=0.5)}})^3}{27\frac{dV}{dG_L}} \tag{3.12}$$

Manipulating equation 3.12 and using equations 2.17 and 2.19 gives:

$$P_{Lmax} = -\frac{1}{27} P_{L_{Pidx=0.5}} P_{idx_{starting\ point}} \frac{\left(2+P_{idx_{starting\ point}}\right)^3}{P_{idx_{starting\ point}}} \quad 3.13$$

Equation 3.13 can be expressed in term of loading multiplier λ as follows

$$\lambda_{max} = \frac{1}{27} \lambda_{Pidx=0.5}\ P_{idx_{starting\ point}} \frac{\left(2 + P_{idx_{starting\ point}}\right)^3}{P_{idx_{starting\ point}}} \quad 3.14$$

Equation 3.14 along with equation 3.10 gives a prediction for point of voltage collapse.

It is worth mentioning that the assumption of a linear relationship between voltage and load conductance is not always valid. However, it is justified for a small portion of the curve. Hence the closer the starting point to the point of voltage collapse the more accurate the prediction [14]. Figure 3.1 shows the actual relationship between the voltage and the load conductance of bus 14 in the IEEE 14-Bus System.

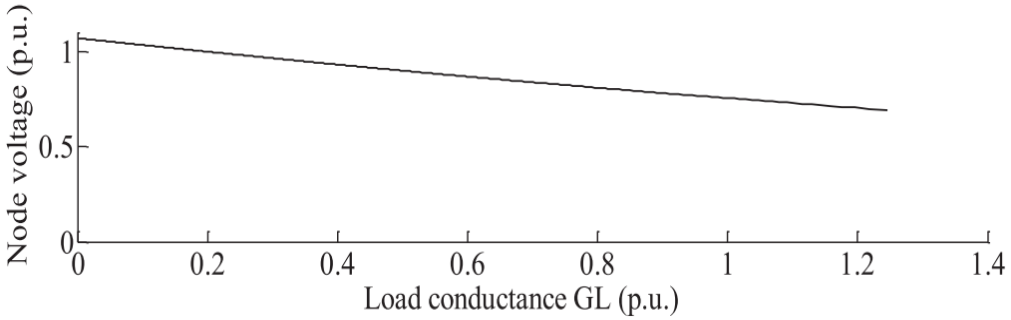

Figure 3.1 Actual V-GL Relationship of Bus 14 in the IEEE 14-Bus System

3.2 Prediction Correction Using Continuation Method

After this Prediction is made it is corrected using a continuation method that uses local parameterization similar to the one discussed in section 2.4. The continuation parameter is chosen as the voltage of the load bus that has the biggest P-index i.e. the critical bus at the starting point (which is the point with the P-index=0.5 for this work). The loading parameter is added as a system variable and the following equation is added to the power flow equations:

$$V_{critical\ bus} = V_{Pidx=0.5} \tag{3.15}$$

Where $V_{critical\ bus}$ is the system variable for the voltage of the critical bus and $V_{Pidx=0.5}$ is the value of that system variable at the starting condition (at P-index=0.5 for this work). As a result of this the conventional Jacobian matrix is augmented by an additional column and row. The additional column represents the relationship between the original system variables and the new variable λ. The active and reactive power equations for a certain bus i are given by:

$$P(i) = P_g - \lambda \mathrm{P_d} \tag{3.16}$$

$$Q(i) = Q_g - \lambda \mathrm{Q_d} \tag{3.17}$$

Where P_g and Q_g are the generated active and reactive power fed into the bus, and $\mathrm{P_d}$ and $\mathrm{Q_d}$ are the load active and reactive power drawn from the bus. Taking the derivative of equations 3.16 and 3.17 with respect to the loading multiplier λ yields:

$$\frac{\partial P(i)}{\partial \lambda} = -\mathrm{P_d} \tag{3.18}$$

$$\frac{\partial Q(i)}{\partial \lambda} = -\mathrm{Q_d} \tag{3.19}$$

The additional row is zeros in every entry except for the continuation parameter entry which is set to be 1. As stated earlier the continuation parameter is selected to be the critical bus voltage. These additions yield the following Jacobian matrix:

$$J = \begin{bmatrix} \frac{\partial P_i}{\partial \delta_k} & \frac{\partial P_i}{\partial V_k} & \frac{\partial P_i}{\partial \lambda} \\ \frac{\partial Q_i}{\partial \delta_k} & \frac{\partial Q_i}{\partial V_k} & \frac{\partial Q_i}{\partial \lambda} \\ & e_k & \end{bmatrix} \tag{3.20}$$

Where e_k is a row vector that has suitable dimensions, and all its elements are zero except for that corresponding to the continuation parameter which is set to 1.

The mismatch vector is also adjusted to accommodate the additional equation by adding an entry with a value of zero.

The adjusted equations are then solved numerically using standard Newton-Raphson based power flow solution technique.

3.3 Updating Prediction Using Two Methods.

The results of the correction process yield another point on the nose curve. This point is used as a starting point for another prediction based on equation 3.14. Another method for

predicting the point of voltage collapse is using equation 2.29. It was shown in [16] that the constants a, b and c can be calculated using the first, and second derivative of V with respect to G_L. However, in this work, these constants are calculated using the two points on the nose curve. The first point is the starting point (G_{L_1}, V_1) when the P-index = 0.5, and the second one is the point obtained from the correction step (G_{L_2}, V_2). Taking the derivative of equation 2.29 yields:

$$\frac{dV}{dG_L} = \frac{-a(b + 2cG_L)}{2(1 + bG_L + cG_L^2)^{\frac{3}{2}}} \tag{3.21}$$

Plugging the aforementioned points into equations 2.29 yields:

$$V_1^2 = \frac{a^2}{1 + bG_{L_1} + cG_{L_1}^2} \tag{3.22}$$

$$V_2^2 = \frac{a^2}{1 + bG_{L_2} + cG_{L_2}^2} \tag{3.23}$$

Dividing equations 3.22 and 3.23 gives

$$s = \frac{1 + bG_{L_2} + cG_{L_2}^2}{1 + bG_{L_1} + cG_{L_1}^2} \tag{3.24}$$

Where

$s = \frac{V_1^2}{V_2^2}$

Rearranging equation 3.24 gives

$$b = \frac{1-s}{sG_{L_1} - G_{L_2}} + \frac{G_{L_2}^2 - sG_{L_1}^2}{sG_{L_1} - G_{L_2}} c \tag{3.25}$$

Let $b_{11} = \frac{1-s}{sG_{L_1} - G_{L_2}}$, and $b_{22} = \frac{G_{L_2}^2 - sG_{L_1}^2}{sG_{L_1} - G_{L_2}}$, equation 3.25 becomes

$$b = b_{11} + b_{22} c \tag{3.26}$$

Now, plugging the starting point into equation 3.21

$$\frac{dV_1}{dG_{L_1}} = \frac{-a(b + 2cG_{L_1})}{2\left(1 + bG_{L_1} + cG_{L_1}^2\right)^{\frac{3}{2}}} \tag{3.27}$$

Dividing equation 3.22 by 3.27

$$\frac{V_1}{\frac{dV_1}{dG_{L_1}}} = \frac{2\left(1 + bG_{L_1} + cG_{L_1}^2\right)^{\frac{3}{2}}}{-(b + 2cG_{L_1})\left(1 + bG_{L_1} + cG_{L_1}^2\right)^{\frac{1}{2}}} \tag{3.28}$$

Let $r = \frac{V_1}{\frac{dV_1}{dG_{L_1}}}$ equation 3.26 becomes

$$r = \frac{2 + 2G_{L_1} b + 2G_{L_1}^2 c}{-b - 2G_{L_1} c} \tag{3.29}$$

Plugging equation 3.26 and rearranging, equation 3.29 becomes

$$-\left(rb_{22} + 2rG_{L_1} + 2G_{L_1} b_{22} + 2G_{L_1}^2\right)c = 2 + rb_{11} + 2G_{L_1} b_{11} \tag{3.30}$$

Hence the constant c can be given by

$$c = \frac{2 + rb_{11} + 2G_{L_1}b_{11}}{-\left(rb_{22} + 2rG_{L_1} + 2G_{L_1}b_{22} + 2G_{L_1}^2\right)} \quad 3.31$$

Once the constant c is obtained, the constant b can be calculated using equation 3.26. Finally constant a can be evaluated using either equation 3.22 or 3.23

$$a = V_1 \left(1 + bG_{L_1} + cG_{L_1}^2\right)^{\frac{1}{2}} \quad 3.32$$

$$or\ a = V_2 \left(1 + bG_{L_2} + cG_{L_2}^2\right)^{\frac{1}{2}} \quad 3.33$$

Once the 3 constants are calculated, equations 2.30 to 2.32 can be used to predict the loading multiplier and the critical bus voltage at point of voltage collapse.

3.4 Generators Reactive Power Limits

In this work the generator reactive power limits are accommodated for in the power flow solution at the starting point and in the correction step. However, if a generator reach its limit between the correction point and the point of collapse it will not be taken into consideration. That being said, the distance between the correction point and the point of voltage collapse is small and the probability of multiple generators reaching their reactive power limits is low and will not affect the loadability margin of the system.

CHAPTER 4

RESULTS AND DISCUSSION

The methods discussed in the previous chapter were implemented in the MATLAB environment and tested on the standard IEEE 14, 57,118, and 300 Bus Systems. The point of voltage collapse was estimated in each system for different conditions with and without respecting the generators reactive power limits. In each case the system loading was increased until the maximum P-index hit 0.5. The bus with the highest P-index is the critical bus, and the voltage collapse point was estimated for that bus using the two proposed methods. The results are presented in the following sections.

4.1 Results for Tests without Generators Reactive Limits

4.1.1 IEEE 14-Bus System

The proposed methods were tested on the intact IEEE-14 Bus System along with some selected outages. Figure 4.1 shows a diagram of the considered system. Table 4.1 summarizes the results obtained from the script.

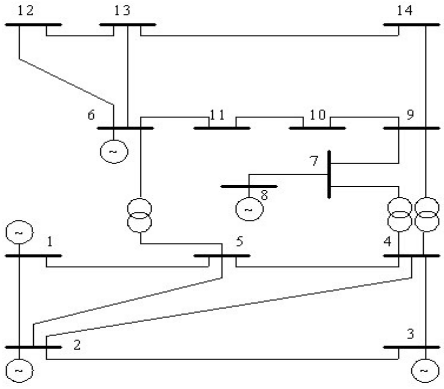

Figure 4.1 IEEE 14-Bus System

Table 4.1 Comparison between the Proposed Methods, Linear Method and Second Derivative Method for the IEEE 14-Bus System without Considering Reactive Limits

Case	λ_m (Actual)	λ_m (Linear Method)	Error (%)	λ_m (Second Derivative Method)	Error (%)	λ_m (Linear-Correction)	Error (%)	λ_m (Quadratic estimation)	Error (%)
Intact	4.040	3.883	3.9	4.174	-3.3	4.033	0.2	4.09	-1.2
1-2 Out	1.343	1.489	-10.8	1.370	-2.0	1.380	-2.8	1.39	-3.5
1-5 Out	3.658	3.583	2.0	3.645	0.3	3.648	0.3	3.65	0.2
2-3 Out	2.268	2.416	-6.5	2.318	-2.2	2.194	3.3	2.3	-1.4
2-4 Out	3.289	3.214	2.3	3.266	0.7	3.278	0.3	3.28	0.3
2-5 Out	3.429	3.327	3.0	3.396	1.0	3.413	0.5	3.42	0.3
3-4 Out	3.944	3.799	3.7	4.074	-3.3	3.938	0.1	3.99	-1.2
4-5 Out	3.940	3.742	5.0	4.113	-4.4	3.935	0.1	4.03	-2.3
4-7 Out	3.604	3.489	3.2	3.720	-3.2	3.602	0.1	3.64	-1.0
4-9 Out	3.942	3.731	5.4	4.058	-2.9	3.927	0.4	4.0	-1.5
5-6 Out	2.283	2.422	-6.1	2.341	-2.5	2.194	3.9	2.33	-2.1
6-11 Out	3.528	2.989	15.3	3.366	4.6	3.311	6.1	3.42	3.1
6-12 Out	3.981	3.718	6.6	4.059	-2.0	3.955	0.6	4.02	-1.0
6-13 Out	3.224	2.773	14.0	3.152	2.2	3.073	4.7	3.18	1.4
7-9 Out	2.876	2.554	11.2	2.827	1.7	2.785	3.2	2.85	0.9
9-10 Out	4.008	3.768	6.0	4.052	-1.1	3.975	0.8	4.03	-0.5
9-14 Out	3.702	3.248	12.3	3.690	0.3	3.580	3.3	3.7	0.1
10-11 Out	3.736	3.284	12.1	3.611	3.4	3.581	4.1	3.66	2.0
12-13 Out	4.029	3.825	5.1	4.136	-2.6	4.014	0.4	4.08	-1.3
13-14 Out	3.245	2.756	15.1	3.132	3.5	3.063	5.6	3.18	2.0

The Quadratic estimation method provided the least error for the vast majority of the cases with a maximum error of 3.5% in the case of line 6-11 outage. By comparison, the linear method had a maximum error of 15.3%, the second derivative method had a maximum error of 4.6%, and the Linear-Correction method maximum error was 6.1%. Table 4.2 provides a statistical analysis of all four methods performance.

Table 4.2 Statistical Analysis of Methods Performance for the IEEE 14-Bus System without Considering Reactive Limits

Method	Linear	Second Derivative	Linear-Correction	Quadratic estimation
Mean Error	7.5	2.3	2.0	1.4
Standard Deviation	4.1	1.2	2.0	0.9
Max Error	15.3	4.6	6.1	3.5
Min Error	2.0	0.3	0.1	0.1

4.1.2 IEEE 57-Bus System

The proposed methods were tested on the intact IEEE-57 Bus System along with some selected outages. Figure 4.2 shows a diagram of the considered system. Table 4.3 summarizes the results obtained from the script.

Table 4.3 Comparison between the Proposed Methods, Linear Method and Second Derivative Method for the IEEE 57-Bus System without Considering Reactive Limits

Case	λ_m (Actual)	λ_m (Linear Method)	Error (%)	λ_m (Second Derivative Method)	Error (%)	λ_m (Linear-Correction)	Error (%)	λ_m (Quadratic estimation)	Error (%)
Intact	1.844	1.497	18.8	1.776	3.7	1.7	7.8	1.8	2.5

1-15 Out	1.803	1.462	18.9	1.740	3.5	1.66	7.9	1.76	2.4
7-29 Out	1.2	1.049	12.6	1.127	6.1	1.1	8.3	1.13	5.9
13-14 Out	1.818	1.474	18.9	1.750	3.7	1.67	8.1	1.77	2.5
22-38 Out	1.632	1.341	17.9	1.584	2.9	1.51	7.5	1.6	1.9
23-24 Out	1.676	1.386	17.3	1.631	2.7	1.56	6.9	1.65	1.7
24-26 Out	1.6344	1.334	18.4	1.581	3.3	1.51	7.6	1.6	2.2
37-38 Out	1.24	1.058	14.7	1.159	6.5	1.12	9.7	1.16	6.1

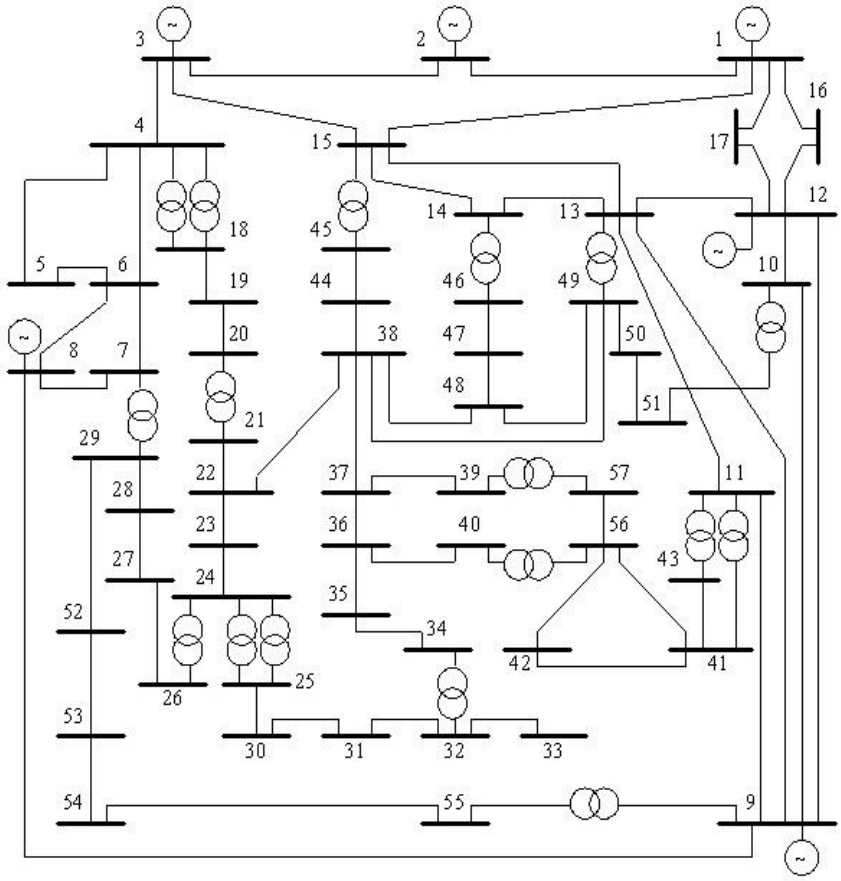

Figure 4.2 IEEE 57-Bus System

The Quadratic estimation method provided the least error for the vast majority of the cases with a maximum error of 6.1%. By comparison, the linear method had a maximum error of 18.9%,

the second derivative method had a maximum error of 6.5%, and the Linear-Correction method maximum error was 9.7%. Table 4.4 provides a statistical analysis of all four methods performance.

Table 4.4 Statistical Analysis of Methods Performance for the IEEE 57-bus System without Considering Reactive Limits

Method	Linear	Second Derivative	Linear-Correction	Quadratic estimation
Mean Error	17.2	4.1	8	3.15
Standard Deviation	2.2	1.3	0.8	1.7
Max Error	18.9	6.5	9.7	6.1
Min Error	12.6	2.7	6.9	1.7

4.1.3 IEEE 118-Bus System

The proposed methods were tested on the intact IEEE-118 Bus System along with some selected outages. Figure 4.3 shows a diagram of the concerned system. Table 4.5 summarizes the results obtained from the script.

Table 4.5 Comparison between the Proposed Methods, Linear Method and Second Derivative Method for the IEEE 118-Bus System without Considering Reactive Limits

Case	λ_m (Actual)	λ_m (Linear Method)	Error (%)	λ_m (Second Derivative Method)	Error (%)	λ_m (Linear-Correction)	Error (%)	λ_m (Quadratic estimation)	Error (%)
Intact	3.200	3.244	-1.4	3.262	-1.9	3.19	0.3	3.19	0.3
26-30 Out	2.610	2.410	7.7	2.615	-0.2	2.59	0.8	2.64	-1.1
49-69 Out	3.190	3.295	-3.3	3.277	-2.7	3.19	0	3.17	0.6
23-24 Out	2.980	3.084	-3.5	3.052	-2.4	2.98	0	2.96	0.7

68-69 Out	2.760	2.966	-7.5	2.782	-0.8	2.74	0.7	2.71	1.8

The Linear-Correction method provided the least error for the vast majority of the cases with a maximum error of 0.8%. By comparison, the linear method had a maximum error of 7.7%, the second derivative method had a maximum error of 2.7%, and the Quadratic estimation method maximum error was 1.8%. Table 4.6 provides a statistical analysis of all four methods performance.

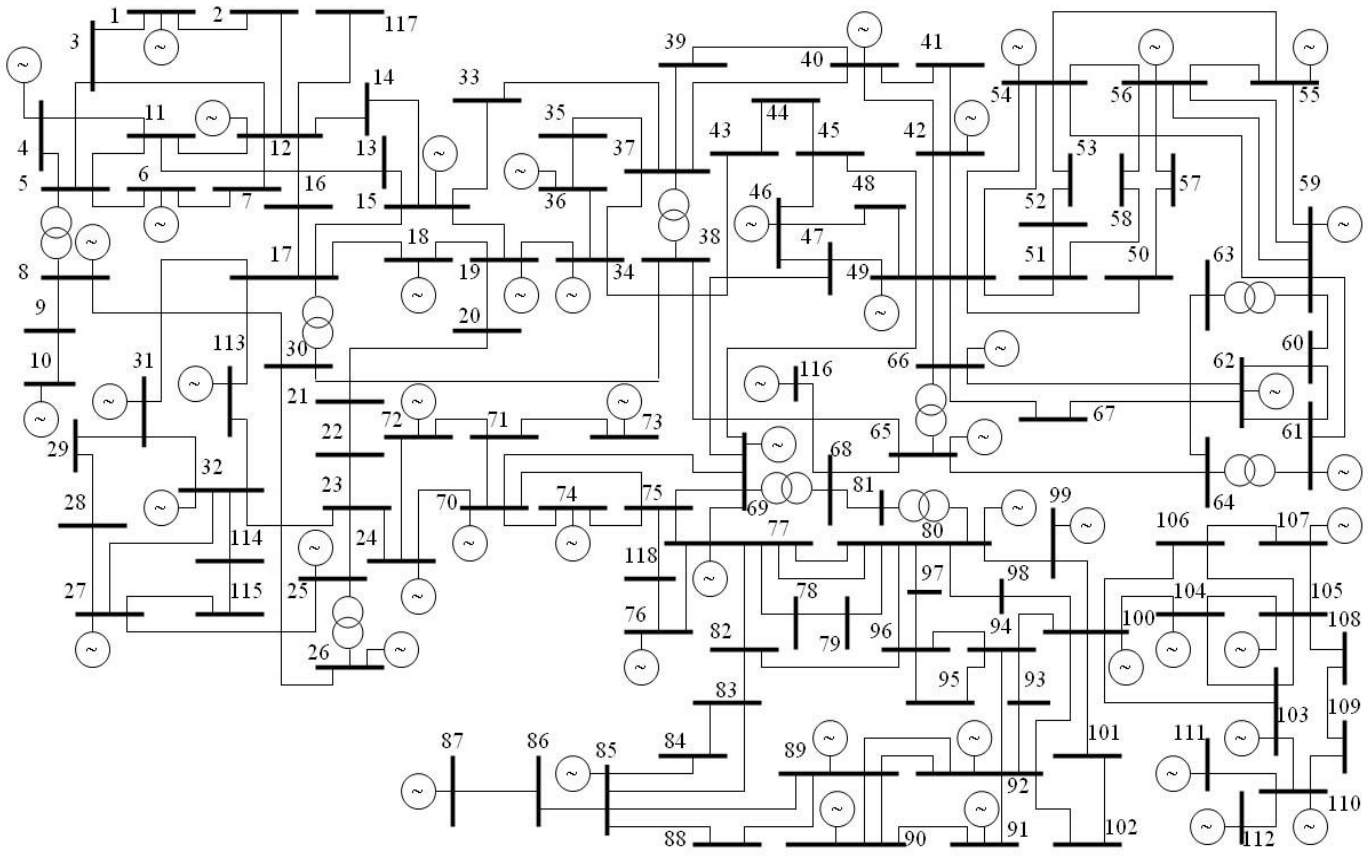

Figure 4.3 IEEE 118-Bus System

Table 4.6 Statistical Analysis of Methods Performance for the IEEE 118-Bus System without Considering Reactive Limits

Method	Linear	Second Derivative	Linear-Correction	Quadratic estimation
Mean Error	4.7	1.6	0.4	0.9
Standard Deviation	2.5	1.0	0.3	0.52
Max Error	7.7	2.7	0.8	1.8
Min Error	1.4	0.2	0	0.3

4.1.4 Testing the methods on the IEEE 300-bus system

The proposed methods were tested on the intact IEEE-300 Bus System along with some selected outages. Figure 4.4 shows a diagram of the concerned system. Table 4.7 summarizes the results obtained from the script.

Table 4.7 Comparisons between the Proposed Methods, Linear Method and Second Derivative Method for the IEEE 300-Bus System without Considering Reactive Limits

Case	λ_m (Actual)	λ_m (Linear Method)	Error (%)	λ_m (Second Derivative Method)	Error (%)	λ_m (Linear-Correction)	Error (%)	λ_m (Quadratic estimation)	Error (%)
Intact	1.430	1.340	6.3	1.445	-1.0	1.44	-0.5	1.46	-2
3-4 Out	1.430	1.273	11.0	1.367	4.4	1.37	4.3	1.39	3
40-68 Out	1.354	1.279	5.5	1.352	0.1	1.34	0.9	1.35	0.1
116-119 Out	1.424	1.275	10.5	1.361	4.4	1.36	4.3	1.38	3.3

The Quadratic estimation provided the least error for the majority of the cases with a maximum error of 3.3%. Linear method had a maximum error of 11%, the second derivative

method had a maximum error of 4.4%, and the Linear-Correction method maximum error was 4.3%. Table 4.8 provides a statistical analysis of all four methods performance.

Table 4.8 Statistical Analysis of Methods Performance for the IEEE 300-Bus System without Considering Reactive Limits

Method	Linear	Second Derivative	Linear-Correction	Quadratic estimation
Mean Error	8.3	2.5	2.5	2.1
Standard Deviation	2.4	1.9	1.8	1.25
Max Error	11.0	4.4	4.3	3.3
Min Error	5.5	0.1	0.5	0.1

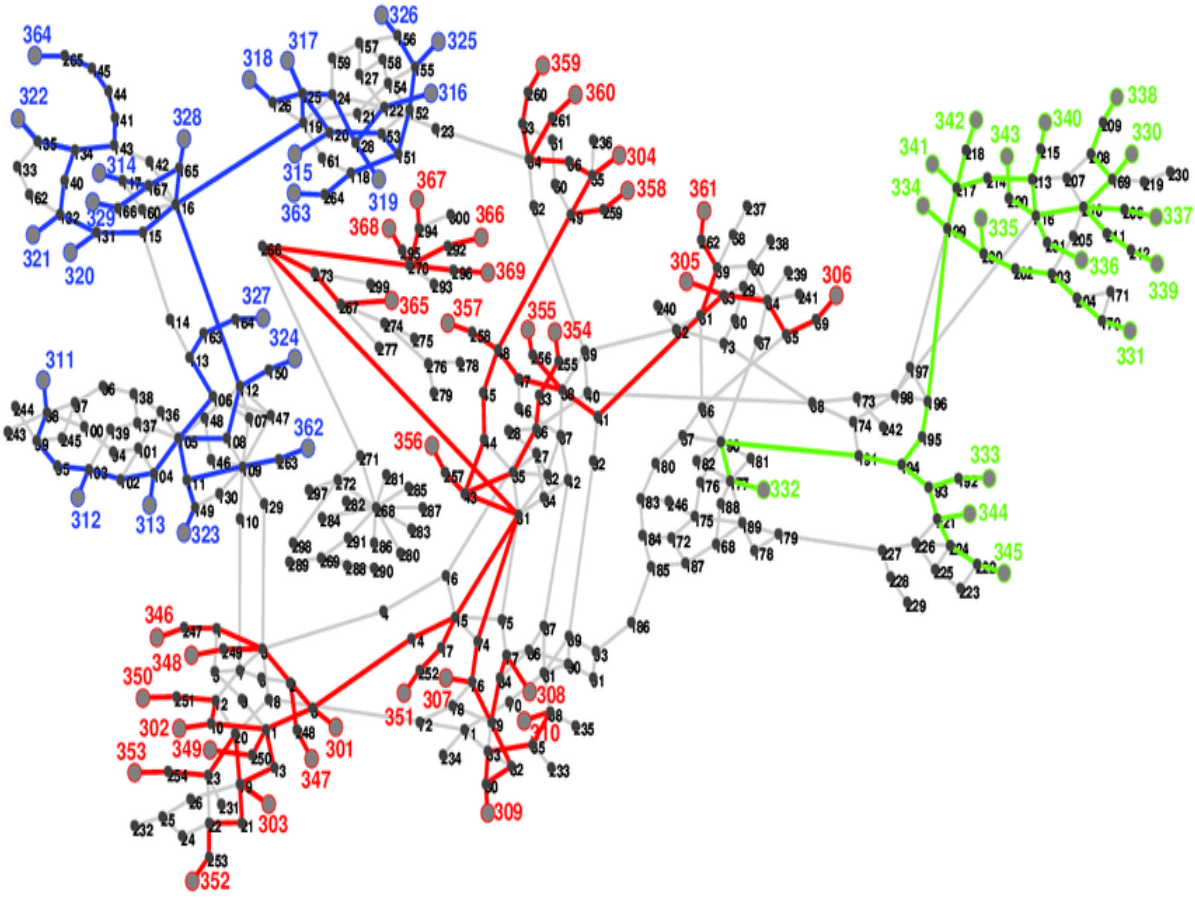

Figure 4.4 IEEE 300-Bus System

4.2 Results for Tests with Generators Reactive Limits

4.2.1 IEEE 14-Bus System

The proposed methods were tested on the intact IEEE-14 Bus System along with some selected outages. Table 4.9 summarizes the results obtained from the script.

Table 4.9 Comparison between the Proposed Methods, Linear Method and Second Derivative Method for the IEEE 14-Bus System with Considering Reactive Limits

Case	λ_m (Actual)	λ_m (Linear Method)	Error (%)	λ_m (Second Derivative Method)	Error (%)	λ_m (Linear-Correction)	Error (%)	λ_m (Quadratic estimation)	Error (%)
Intact	1.766	1.566	11.3	1.741	1.4	1.74	1.5	1.69	4.3
1-5 Out	1.388	1.235	11.0	1.370	1.3	1.34	3.5	1.3	6.3
2-4 Out	1.292	1.204	6.8	1.297	-0.4	1.55	1.9	1.51	4.4
2-5 Out	1.580	1.406	11.0	1.560	1.3	1.62	1.8	1.57	4.8
4-5 Out	1.649	1.464	11.2	1.627	1.3	1.57	2.4	1.53	4.9
4-7 Out	1.609	1.445	10.2	1.593	1.0	1.57	0.3	1.54	2.2
4-9 Out	1.575	1.400	11.1	1.558	1.1	1.66	1	1.63	2.7
6-13 Out	1.676	1.483	11.5	1.652	1.4	1.65	0.2	1.62	2.1
9-14 Out	1.654	1.428	13.7	1.616	2.3	1.57	4.6	1.53	7
12-13 Out	1.645	1.400	14.9	1.597	2.9	1.73	1.9	1.69	4.2

The proposed methods provide results with less error than the linear method, and similar errors to the second derivative method. Table 4.10 provides a statistical analysis of all four methods performance for this system.

Table 4.10 Statistical Analysis of Methods Performance for the IEEE 14-Bus System while Considering Reactive Limits

Method	Linear	Second Derivative	Linear-Correction	Quadratic estimation
Mean Error	11.1	1.4	1.9	4.29
Standard Deviation	1.9	0.7	1.3	1.54
Max Error	14.9	2.9	4.6	7
Min Error	6.8	0.4	0.2	2.1

Since there were no generator that hit their reactive limit between the starting point and critical point; the second derivative methods provided the best results but it is comparable to the proposed methods. However, when generators hit their reactive limit after the starting point and before the critical point the second derivative method gives notably higher error than the proposed methods as seen in the IEE 57-bus system discussed next.

4.2.2 IEEE 57-Bus System

The proposed methods were tested on the intact IEEE-57 Bus System along with some selected outages. Table 4.11 summarizes the results obtained from the script.

Table 4.11 Comparison between the Proposed Methods, Linear Method and Second Derivative Method for the IEEE 57-Bus System with Considering Reactive Limits

Case	λ_m (Actual)	λ_m (Linear Method)	Error (%)	λ_m (Second Derivative Method)	Error (%)	λ_m (Linear-Correction)	Error (%)	λ_m (Quadratic estimation)	Error (%)
Intact	1.439	1.351	6.1	1.581	-9.9	1.45	-0.9	1.42	1.5
23-24 Out	1.442	1.307	9.4	1.523	-5.6	1.41	2.1	1.41	2.5
13-14 Out	1.451	1.346	7.2	1.573	-8.4	1.43	1.4	1.42	2.3

22-38 Out	1.446	1.324	8.4	1.567	-8.4	1.43	1.1	1.48	-2.4
24-26 Out	1.407	1.238	12.0	1.433	-1.8	1.42	-0.9	1.45	-2.9

As mentioned above, some generators in this system reach their limits between the starting point and the critical point. This makes the second derivative method less accurate (6.2% average error). However, the correction step in the proposed methods gives a point further on the nose curve and takes the reactive power limits into consideration. This makes the proposed methods more accurate in these situations (1.28% and 2.32% average error). Table 4.12 provides a statistical analysis of all four methods performance for this system.

Table 4.12 Statistical Analysis of Methods Performance for the IEEE 57-bus System while Considering Reactive Limits

Method	Linear	Second Derivative	Linear-Correction	Quadratic estimation
Mean Error	8.4	6.2	1.3	2.32
Standard Deviation	1.8	3.4	0.5	0.46
Max Error	12.0	9.9	2.1	2.9
Min Error	6.1	0.3	0.9	1.5

4.2.3 IEEE 300-Bus System

The proposed methods were tested on the intact IEEE-300 Bus System along with some selected outages. Table 4.13 summarizes the results obtained from the script.

Table 4.13 Comparison between the Proposed Methods, Linear Method and Second Derivative Method for the IEEE 300-Bus System with Considering Reactive Limits

Case	λ_m (Actual)	λ_m (Linear Method)	Error (%)	λ_m (Second Derivative Method)	Error (%)	λ_m (Linear-Correction)	Error (%)	λ_m (Quadratic estimation)	Error (%)
Intact	1.058	1.087	-2.7	1.099	-3.9	1.0027	5.2	1.0031	5.2
3-4 Out	1.009	1.058	-4.9	1.069	-5.9	1	0.9	1	0.9
40-68 Out	1.025	1.051	-2.5	1.064	-3.8	1.0044	2	1.0004	2.4

The IEEE 300-Bus System is heavily stressed with a small margin of loadability. This makes the predictions very sensitive and hence unreliable as the margin of error overshadow these sensitivities. Table 4.14 provides a statistical analysis of all three methods performance for this system.

Table 4.14 Statistical Analysis of Methods Performance for the IEEE 300-Bus System while Considering Reactive Limits

Method	Linear	Second Derivative	Linear-Correction	Quadratic estimation
Mean Error	3.4	4.5	2.7	2.83
Standard Deviation	1.0	1.0	1.8	1.78
Max Error	4.9	5.9	5.2	5.2
Min Error	2.5	3.8	0.9	0.9

4.3 Performance Comparisons

The performance of the proposed methods was compared to the second derivative method and the direct computation method that was proposed in [15]. Tables 4.15 and 4.16 provide a time comparison between the proposed methods and the aforementioned methods.

Table 4.15 Time Comparison between the Different Approaches when Neglecting Reactive Power Limits

System\Method	Correction Methods (s)	Second Derivative (s)	Direct Computation (s)
IEEE 14-Bus	0.005	0.06	0.001
IEEE 57-Bus	0.033	0.07	0.303
IEEE 118-Bus	0.78	0.14	0.54
IEEE 300-Bus	1.2	0.25	4.1

Table 4.16 Time Comparison between the Different Approaches when Considering Reactive Power Limits

System\Method	Correction Methods (s)	Second Derivative (s)	Direct Computation (s)
IEEE 14-Bus	0.01	0.06	0.03
IEEE 57-Bus	0.04	0.10	0.49
IEEE 300-Bus	0.5	0.4	1 min

The proposed methods give accurate results and as shown in the previous sections, and its computational time is comparable to the second derivative method, and sometimes they outperform it. It is worth mentioning that the majority of the computational time is spent in the correction step. The correction step is very dependent on the initial state of the system i.e. the starting point. The number of iterations needed for the convergence depends on the initial state.

CHAPTER 5

CONCLUSION AND FUTURE WORK

5.1 Conclusion

This work proposed a new method for the estimation of the point of voltage collapse. The new methods starts from a known system conditions, and makes an estimation of the point of voltage collapse based on an assumption of linearity between voltage and load conductance. This estimation is then corrected by continuation scheme. From the results of the correction step it gives two estimations, one assumes the aforementioned linearity and the other dose not.

The proposed methods were tested on the standard IEEE 14, 57,118, and 300 Bus Systems with and without respecting the generators reactive power limits. The results are then compared to initial prediction and the second derivative method.

In the majority of the cases the proposed methods gave more accurate and conservative results than the second derivative method without a compromise on computational efficiency. More over the generators reactive power limits are taken into consideration beyond the starting point unlike the second derivative method.

5.2 Future Work

Load modeling influences voltage stability studies, especially voltage-dependent load models. This analysis has assumed a static load model. In practice, loads are more accurately modeled in a dynamic matter through higher order polynomial. A dynamic load models can be introduced, and the proposed methods can be changed to accommodate these models. Moreover motor stalling can be also incorporated in the models, as they also have an effect on voltage stability studies.

REFERENCES

[1] P. Kundur *et al.*, "Definition and classification of power system stability IEEE/CIGRE joint task force on stability terms and definitions," *IEEE Transactions on Power Systems,* vol. 19, no. 3, pp. 1387-1401, 2004, doi: 10.1109/TPWRS.2004.825981.

[2] I. G. Adebayo, A. A. Jimoh, and A. A. Yusuff, "A comparison of voltage collapse point prediction capabilities of voltage stability index and inherent structural characteristics," in *AFRICON 2015*, 14-17 Sept. 2015 2015, pp. 1-5, doi: 10.1109/AFRCON.2015.7331862.

[3] N. S. Group, "Technical analysis of the August 14, 2003, blackout: What happened, why, and what did we learn," *NERC, report to the NERC Board of Trustees*, 2004.

[4] J. M. O. Filho. (2010) Brazilian Blackout 2009. *PAC World Magazine*. 36-37.

[5] P. Kundur , N. J. Balu, and M. Lauby, *Power system stability and control*. New York: McGraw-hill 1994.

[6] M.-S. Chen and H. chungshih, "Reactive Power and Voltage Stability. A short course," ed, 2005, p. 100.

[7] V. Ajjarapu and C. Christy, "The continuation power flow: a tool for steady state voltage stability analysis," in *[Proceedings] Conference Papers 1991 Power Industry Computer Application Conference*, 7-10 May 1991 1991, pp. 304-311, doi: 10.1109/PICA.1991.160593.

[8] K. Vu, M. M. Begovic, D. Novosel, and M. M. Saha, "Use of local measurements to estimate voltage-stability margin," in *Proceedings of the 20th International Conference on Power Industry Computer Applications*, 11 May-16 June 1997 1997, pp. 318-323, doi: 10.1109/PICA.1997.599420.

[9] C. Elizabeth Doig Cardet, *Analysis on Voltage Stability Indices*. Universitat Politècnica de Catalunya. Escola Tècnica Superior d'Enginyeria Industrial de Barcelona. Escola Tècnica Superior d'Enginyeria Industrial de Barcelona, 2010.

[10] P. Lof, T. Smed, G. Andersson, and D. J. Hill, "Fast calculation of a voltage stability index," *IEEE Transactions on Power Systems,* vol. 7, no. 1, pp. 54-64, 1992, doi: 10.1109/59.141687.

[11] A. Berizzi, P. Finazzi, D. Dosi, P. Marannino, and S. Corsi, "First and second order methods for voltage collapse assessment and security enhancement," *IEEE Transactions on Power Systems,* vol. 13, no. 2, pp. 543-551, 1998, doi: 10.1109/59.667380.

[12] A. C. Z. d. Souza, C. A. Canizares, and V. H. Quintana, "New techniques to speed up voltage collapse computations using tangent vectors," *IEEE Transactions on Power Systems,* vol. 12, no. 3, pp. 1380-1387, 1997, doi: 10.1109/59.630485.

[13] P. Kessel and H. Glavitsch, "Estimating the Voltage Stability of a Power System," *IEEE Power Engineering Review,* vol. PER-6, no. 7, pp. 72-72, 1986, doi: 10.1109/MPER.1986.5527889.

[14] M. Kamel, A. A. Karrar, and A. H. Eltom, "Development and Application of a New Voltage Stability Index for On-Line Monitoring and Shedding," *IEEE Transactions on Power Systems,* vol. 33, no. 2, pp. 1231-1241, 2018, doi: 10.1109/TPWRS.2017.2722984.

[15] W. Elballa, A. Karrar, and A. Eltom, "A Novel Optimization Formulation for the Direct Computation of the Voltage Collapse Point," in *2018 IEEE Power & Energy Society General Meeting (PESGM)*, 5-10 Aug. 2018 2018, pp. 1-5, doi: 10.1109/PESGM.2018.8585992.

[16] S. Mohammed, "Improved Computations of the Voltage Collapse Point using the P-Index," The University of Tennessee at Chattanooga 2018.

VITA

Anas Ali was born Sour, Oman in 1992. Before attending The University of Tennessee at Chattanooga as a Master of Science candidate, he attended the University of Khartoum in Khartoum, Sudan, where he earned a Bachelor of Science in Electrical Engineering, with First Class, in 2015. In January 2017, Mr. Ali was awarded a graduate assistantship at The University of Tennessee at Chattanooga. Anas was awarded a Master of Science degree in Electrical Engineering in May 2019.

While at The University of Tennessee at Chattanooga, Anas worked on multiple projects for both Tennessee Valley Authority (TVA), and Electric Power Board (EPB).. Moreover, Anas had a publication in the IEEE 2018 PES General Meeting in Portland, Oregon.